



OPEN

Fuzzy analytic hierarchy process based generation management for interconnected power system

T. Varshney¹, A. V. Waghmare², V. P. Singh², V. P. Meena³, R Anand³ & Baseem Khan^{4✉}

Decision makers consistently face the challenge of simultaneously assessing numerous attributes, determining their respective importance, and selecting an appropriate method for calculating their weights. This article addresses the problem of automatic generation control (AGC) in a two area power system (2-APS) by proposing fuzzy analytic hierarchy process (FAHP), an multi-attribute decision-making (MADM) technique, to determine weights for sub-objective functions. The integral-time-absolute-errors (ITAE) of tie-line power fluctuation, frequency deviations and area control errors, are defined as the sub-objectives. Each of these is given a weight by the FAHP method, which then combines them into a single final objective function. This objective function is then used to design a PID controller. To improve the optimization of the objective function, the Jaya optimization algorithm (JOA) is used in conjunction with other optimization techniques such as sine cosine algorithm (SCA), Luus–Jaakola algorithm (LJA), Nelder–Mead simplex algorithm (NMSA), symbiotic organism search algorithm (SOSA) and elephant herding optimization algorithm (EHOA). Six distinct experimental cases are conducted to evaluate the controller's performance under various load conditions, with data plotted to show responses corresponding to fluctuations in frequency and tie-line exchange. Furthermore, statistical analysis is performed to gain a better understanding of the effectiveness of the JOA-based PID controller. For non-parametric evaluation, Friedman rank test is also used to validate the performance of the proposed JOA-based controller.

Keywords Fuzzy AHP, AHP, Jaya optimization algorithm, PID controller, AGC, Power system

Decision making is inherently complex and frequently requires the simultaneous consideration of multiple factors as well as expert judgment¹. Because of this, the strategic identification of key factors becomes imperative. Analytic hierarchy process (AHP) has become a popular method for handling multi-attribute decision-making (MADM) scenarios. The reasons for the widespread use of AHP are:

- Its ease of use.
- Flexibility in incorporating a wide range of variables with quantitative and qualitative characteristics.
- Wide application in different fields.
- Accessibility of auxiliary software.

Parekh et al. demonstrated use of AHP to determine the relative importance of each performance indicator for solid waste management (SWM) in². A land susceptibility model is developed in³ using AHP where relative weights of all landslip instability factors are determined with the help of AHP. AHP technique, along with GIS-based ranking were used in⁴ for finding the best locations in Kayseri, Turkey for solar photovoltaic (PV) power plant construction. Similar to this, Hammami et al. in⁵ also applied AHP technique along with GIS based multi-criteria decision analysis in flood susceptibility mapping at Tunisia. In⁶, based on AHP, the expert evaluation matrix is optimised using the accelerating genetic algorithm to determine the subjective weights. Nyimbili integrated AHP with TOPSIS and GIS techniques in⁷ for analyzing earthquake hazards. In⁸, weights of groundwater indicators, which are used for groundwater quality evaluation, were determined using AHP.

¹Department of EECE, SSET, Sharda University, Greater Noida, Uttar Pradesh 201310, India. ²Department of Electrical Engineering, Malaviya National Institute of Technology, Jaipur, Rajasthan 302017, India. ³Department of Electrical and Electronics Engineering, Amrita School of Engineering, Bengaluru, Amrita Vishwa Vidyapeetham, Bengaluru, India. ⁴Department of Electrical and Computer Engineering, Hawassa University, Hawassa, Ethiopia. ✉email: baseem.khan04@gmail.com

In spite of all the advantages of the AHP technique, the realization that traditional AHP has trouble in adequately addressing uncertainty⁹, especially when decision-makers are limited to a predetermined rating system from 1 to 9. This led to the adoption of fuzzy AHP (FAHP). FAHP is a derivative of AHP that has gained popularity recently and combines AHP with fuzzy set theory. Decision-makers have more freedom to have more flexible scales that use fuzzy membership functions and linguistic variables rather than deterministic or precise values in order to effectively capture uncertainty.

Many researchers have opted FAHP methods for decision making. Ertuğrul et al. in¹⁰ used FAHP technique for weight determination in facility location selection process. In¹¹, FAHP is used in determining weights of machine tool alternatives for multiple attributes. Shaygan, in¹², illustrated an actual implementation of FAHP method for identifying, ranking, and choosing enhancement projects for a hospital's under performing appointment system. In¹³, FAHP method is implemented to fully structured decision-making problems involving alternatives, sub-criteria, and criteria for evaluating water management plans in a section of Brazil's Paraguacu river basin. In¹⁴, three potential landfill locations for Istanbul are assessed using FAHP in addition to expert opinion. Similarly, Karasan et al. in¹⁵ implemented novel pythagorean FAHP method landfill site selection problem.

MADM techniques like rank sum weight, AHP and rank exponent are implemented for AGC problem of 2-APS in the literature^{16–19}. AGC ensures maintaining the overall power balance of the system that is dependent on critical factors such as frequency deviation, area control errors, and tie-line power deviation^{20,21}. The controllers used in AGC play an important role in correcting system imbalances^{22–24}. It is critical to optimize the parameters of these controllers to ensure a consistent and efficient flow of power. When designing controllers, choosing an appropriate objective function is necessary for improving and optimizing^{25,26} parameter changes. This objective function typically includes sub-objective functions that represent error indices for frequency deviation, area control errors, and tie-line power deviation. Prioritizing sub-objective functions and assigning appropriate ranks and weights are critical in attaining an optimal outcome for the objective function. As a result, once the weights are properly determined, additional step involving optimization^{27–30} of the objective function is required.

In this paper, FAHP technique is implemented for AGC problem of 2-APS. This technique is used to provide weights corresponding to sub-objective functions, which are further utilized to tune PID controller. For sub-objective functions, the ITAE evaluations of the frequency deviations, control errors, and tie-line power deviation for the AGC problem of 2-APS are taken into account. The PID controller design utilizes each of these sub-objective functions. Subsequently all weighted sub-objectives are combined to create the objective function and further Jaya optimization algorithm (JOA)^{31–33} is used to minimize the same. Six different experimental cases are used to evaluate the FAHP's effectiveness. Additionally, sine cosine algorithm (SCA), Luus–Jaakola algorithm (LJA), Nelder–Mead simplex algorithm (NMSA), symbiotic organism search algorithm (SOSA) and elephant herding optimization algorithm (EHOA) are used in optimization to demonstrate the effectiveness of the JOA algorithm-based controller. The results are compared for each of the six load variations, and both tabular and graphical comparisons are displayed. Comparisons are made on the basis of specifications such as peak overshoots, settling times, decision parameters, and values of the objective function. A statistical analysis is performed by evaluating mean, minimum, maximum, and standard deviation values of the objective function obtained from JOA, SCA, LJA, NMSA, SOSA, and EHOA. Friedman rank test is used to further elucidate the effectiveness and accuracy of the results obtained. By assigning a mean rank to each of the six algorithms and calculating an overall *Q* value and *p* value, this test offers a non-parametric analysis.

The key objectives of this article are as follows:

- FAHP technique is investigated to determine weights of sub-objective functions for AGC problem of 2-APS.
- ITAEs of frequency deviations, tie-line deviations and control errors are considered as sub-objective functions.
- PID controller is designed on the basis of single objective function formed by merging all the weighted sub-objective functions.
- Minimization of objective function is performed using JOA.
- The results obtained from JOA are compared with those obtained from SCA, LJA, NMSA, SOSA and EHOA, by performing statistical analysis and Friedman rank test.

The architecture of this study is structured as follows. Section “[Fuzzy analytic hierarchy process](#)” elaborates the FAHP method in detail. The considered 2-APS is introduced in Sect. “[Considered system](#)”. The implementation of FAHP method to 2-APS is provided in Sect. “[Implementation of FAHP method for AGC problem](#)”. In Sect. “[Jaya optimization algorithm](#)”, Jaya optimization algorithm is explained. In Sect. “[Results and discussions](#)”, the results obtained are discussed in detail. Finally the derived conclusion is presented in Sect. “[Conclusion](#)”.

Fuzzy analytic hierarchy process

Fuzzy analytic hierarchy process (FAHP) is a multi attribute decision making (MADM) technique used to determine weights using fuzzy rules³⁴. On the basis of these fuzzy rules, a decision matrix is formed whose elements denote the performance measure of one decision making problem with respect to other decision making problem. These performance measures are dependant on fuzzy membership function. For defining fuzzy rules, triangular fuzzy membership (TFM)³⁵ function with real numbers are utilized. Let F_{ϕ} be TFM function consisting of triangular fuzzy rules, which is defined in (1).

$$F_\phi = \begin{cases} 0 & \phi < L \\ (\phi - L)/(M - L) & L \leq \phi \leq M \\ (U - \phi)/(U - M) & M \leq \phi \leq U \\ 0 & \phi > U \end{cases} \tag{1}$$

In (1), L, M and U denotes the lower, middle and upper range values of TFM function element. For each fuzzy element of a TFM function, a fuzzy performance index is defined according to its significance level, as given in Table 1.

The detailed procedure involved in determining weights using FAHP is discussed below:

Step 1: Identification of criteria and their relative significances

In FAHP, criteria are needed to be defined for decision making, which are termed as alternatives and attributes. Let there be N alternatives and M attributes. The weights corresponding to attributes are denoted as O_m , where $m = 1, 2, \dots, M$, and those corresponding to alternatives are denoted as O_n , where $n = 1, 2, \dots, N$.

Step 2: Pair-wise decision matrix formulation

After defining the alternatives and attributes, a pair wise decision matrix is formed using TFM function. The elements of matrix are fuzzy element taken from Table 1 and are denoted by P_{mn} and their significance level is decided on the basis of m^{th} attribute's relation with n^{th} alternative. For example, if m^{th} attribute is at "Highest" significance level with respect to n^{th} alternative, then $P_{m,n}$ will be "(8,9,10)" which is considered from Table 1. And if there is no difference in the significance level of m^{th} attribute and n^{th} alternative, then then P_{mn} will be considered as 'Identical' i.e. "(1,1,1)". The representation of decision matrix is given in (2).

$$A = \begin{matrix} & \begin{matrix} O_1 & O_2 & O_3 & \dots & O_N \end{matrix} \\ \begin{matrix} O_1 \\ O_2 \\ O_3 \\ \vdots \\ O_M \end{matrix} & \begin{bmatrix} P_{1,1} & P_{1,2} & P_{1,3} & \dots & P_{1,N} \\ P_{2,1} & P_{2,2} & P_{2,3} & \dots & P_{2,N} \\ P_{3,1} & P_{3,2} & P_{3,3} & \dots & P_{3,N} \\ \vdots & \vdots & \vdots & \ddots & \vdots \\ P_{M,1} & P_{M,2} & P_{M,3} & \dots & P_{M,N} \end{bmatrix} \end{matrix} \tag{2}$$

Fuzzy element $P_{m,n}$ i.e. TFM function is defined such that $P_{m,n} = P_{m,n}^{-1}$ when $m \neq n$ and $P_{m,n} = 1$ when $m = n$.

Step 3: Evaluation of geometric mean

The interval arithmetic for TFM function is utilized to evaluate geometric mean (GM_m) of the m^{th} alternative which is calculated using (3).

$$GM_m = \left[\prod_{n=1}^N P_{m,n} \right]^{1/N} \tag{3}$$

where, GM_m is geometric mean and it shows radical root of m^{th} alternative's in decision matrix.

Step 4: Calculation of fuzzy weights

For respective attributes, relative fuzzy weights (FO_m) are calculated as

$$FO_m = \frac{GM_m}{\sum_{m=1}^M GM_m} \tag{4}$$

Step 5: Calculation of best non-fuzzy performance value as weights

The calculation of best non-fuzzy performance (BNFP) value as weights is done as

Fuzzy	Fuzzy element as a	Significance
Performance index	TFM function	Level
10	(9,10,11)	Absolute
9	(8,9,10)	Highest
8	(7,8,9)	Higher
7	(6,7,8)	High
6	(5,6,7)	Above average
5	(4,5,6)	Average
4	(3,4,5)	Low
3	(2,3,4)	Lower
2	(1,2,3)	Least
1	(1,1,1)	Identical

Table 1. Performance indices with TFM function and their relative significance.

$$O_m = \frac{[FO(L)_m + FO(M)_m + FO(U)_m]}{3} \tag{5}$$

where $FO(L)_m$, $FO(M)_m$ and $FO(U)_m$ represent the lower, middle and upper fuzzy values, respectively, to calculate BNFP value based on fuzzy membership function.

Considered system

A schematic representation of two area power system (2-APS), inspired from³⁶, is provided in Fig. 1. With two thermal power plants contributing 1000 MW each to the overall load, the system configuration includes a combined capacity of 2000 MW. This configuration simulates an actual networked power system. The parameters of 2-APS for area 1, area 2 and tie-line region are described in Table 2, Table 3 and Table 4. The mathematical models of components of 2-APS for area 1 and area 2, in form of transfer functions, are presented in Table 5.

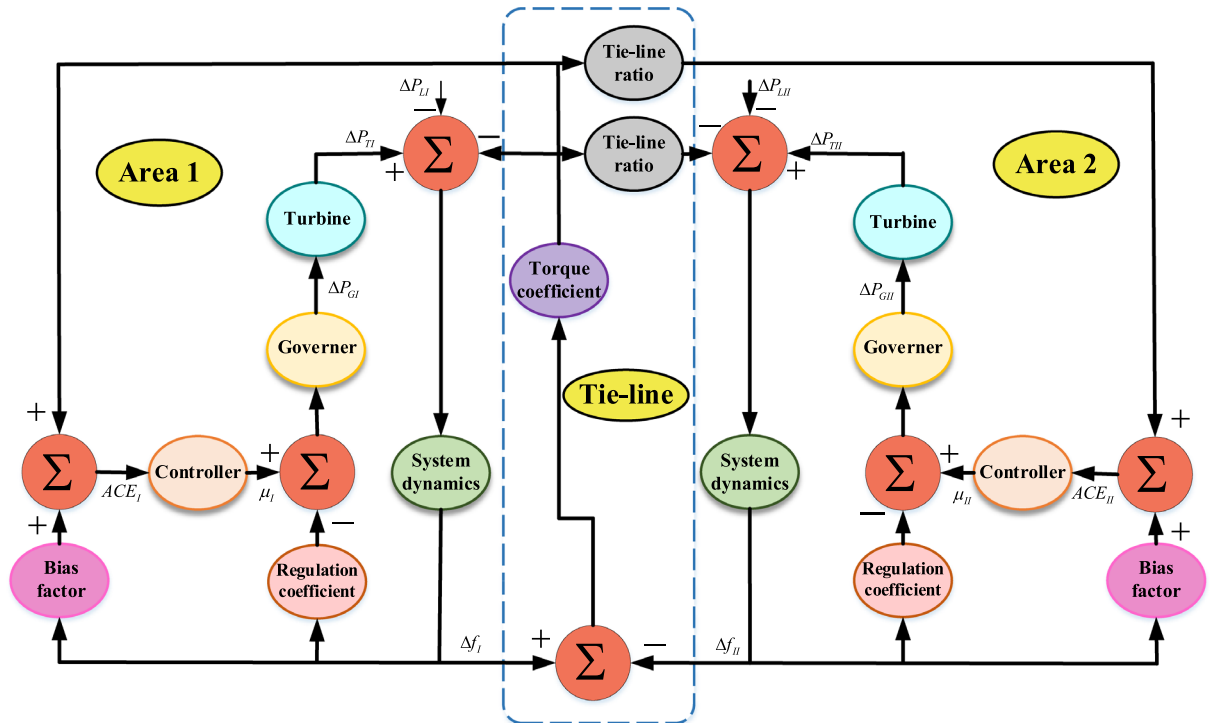


Figure 1. 2-APS.

2-APS parameters (Area 1)		
Parameter	Variable	Value (unit)
Frequency	f	60Hz
Frequency deviation	Δf_I	-
Area control error	ACE_I	-
Bias factor	β_I	0.05pu MW/Hz
Control input	μ_I	-
Governor's speed regulation constant	R_I	2.4Hz/pu
Governor's time constant	τ_{GI}	0.08sec.
Turbine's time constant	τ_{TI}	0.3sec
System's gain constant	K_I	120Hz/pu MW
System's time constant	τ_I	20sec.
Governor power deviation	ΔP_{GI}	-
Turbine power deviation	ΔP_{TI}	-
System's load change	ΔP_{LI}	-

Table 2. 2-APS parameters (Area 1).

2-APS parameters (Area 2)		
Parameter	Variable	Value (unit)
Frequency	f	60Hz
Frequency deviation	Δf_{II}	-
Area control error	ACE_{II}	-
Bias factor	β_{II}	0.05pu MW/Hz
Control input	μ_{II}	-
Governer's speed regulation constant	R_{II}	2.4Hz/pu
Governer's time constant	τ_{GII}	0.08sec.
Turbine's time constant	τ_{TII}	0.3sec
System's gain constant	K_{II}	120Hz/pu MW
System's time constant	τ_{II}	20sec.
Governer power deviation	ΔP_{GII}	-
Turbine power deviation	ΔP_{TII}	-
System's load change	ΔP_{LII}	-

Table 3. 2-APS parameters (Area 2).

2-APS parameters (tie line)		
Parameter	Variable	Value (unit)
Torque coefficient	$T_{tie-line}$	0.545 pu
Tie-line ratio	$A_{tie-line}$	-1
Tie-line power deviation	$\Delta Z_{tie-line}$	-

Table 4. 2-APS parameters (Tie line).

2-APS transfer functions		
Component	Area 1	Area 2
Turbine	$TF_{T1} = \frac{1}{1+s\tau_{T1}}$	$TF_{TII} = \frac{1}{1+s\tau_{TII}}$
Generator	$TF_{G1} = \frac{1}{1+s\tau_{G1}}$	$TF_{GII} = \frac{1}{1+s\tau_{GII}}$
System dynamics	$TF_I = \frac{K_I}{1+s\tau_I}$	$TF_{II} = \frac{K_{II}}{1+s\tau_{II}}$

Table 5. 2-APS transfer functions.

PID controller

PID controllers are extensively used by numerous industries, especially in process industries. Their extensive use is because of their dependability and ease for handling. For the majority of systems, they offer strong and dependable performance as long as the PID parameters are chosen or adjusted to guarantee an acceptable closed-loop performance. PID controller operates on the basis that each of the three terms i.e. proportional, integral, and derivative are supposed to be “tuned” appropriately. An input is subjected to a correction factor i.e. error, which is computed based on the variation between these values. A basic PID controller is mathematically expressed in (6).

$$Y(s) = \Gamma_P * E(s) + \frac{\Gamma_I}{s} * E(s) + \Gamma_D s * E(s) \tag{6}$$

In (6), $Y(s)$ is output signal; Γ_P, Γ_I and Γ_D are proportional, integral, and derivative terms, respectively; and $E(s)$ is error signal. To lessen the effect of noise, the PID controller used in this study integrates a filter F with the derivative gain. The generated outputs are control inputs, μ_I and μ_{II} , and area control errors ACE_I and ACE_{II} are controller inputs. The expressions for μ_I and μ_{II} are presented in (7) and (8).

$$\mu_I(s) = \Gamma_P * ACE_I(s) + \frac{\Gamma_I}{s} * ACE_I(s) + \Gamma_D s \frac{1}{\frac{1}{s} + \frac{1}{F}} * ACE_I(s) \tag{7}$$

$$\mu_{II}(s) = \Gamma_P * ACE_{II}(s) + \frac{\Gamma_{II}}{s} * ACE_{II}(s) + \Gamma_D s \frac{1}{\frac{1}{s} + \frac{1}{F}} * ACE_{II}(s) \tag{8}$$

ACE_I and ACE_{II} from (7) and (8) can be further elaborated as follows:

2-APS parameters (constraints)		
Parameter	Max value	Min value
Proportional gain	$\Gamma_P^{max} = 3$	$\Gamma_P^{min} = 0$
Integral gain	$\Gamma_I^{max} = 3$	$\Gamma_I^{min} = 0$
Derivative gain	$\Gamma_D^{max} = 3$	$\Gamma_D^{min} = 0$
Filter	$F^{max} = 500$	$F^{min} = 0$

Table 6. 2-APS parameters (constraints).

$$ACE_I(s) = \Delta Z_{tie-line}(s) + \beta_I \cdot \Delta f_I(s) \tag{9}$$

$$ACE_{II}(s) = -A_{tie-line} \cdot \Delta Z_{tie-line}(s) + \beta_{II} \cdot \Delta f_{II}(s) \tag{10}$$

Objective function formulation

Maintaining area control errors to minimum values, maintaining tie-line powers, and upholding the frequencies of area 1 and area 2 are essential in ensuring a balanced power flow. Sub-objective functions are developed by taking these three factors into account, which are further clubbed into a single objective function. For this study, ITAEs of aforementioned factors are, respectively, evaluated to determine the sub-objective functions, which are mathematically presented in (11), (12) and (13).

$$OF_I = \int_0^{T_{st}} \Delta f_I t dt + \int_0^{T_{st}} \Delta f_{II} t dt \tag{11}$$

$$OF_{II} = \int_0^{T_{st}} ACE_I t dt + \int_0^{T_{st}} ACE_{II} t dt \tag{12}$$

$$OF_{III} = \int_0^{T_{st}} \Delta Z_{tie-line} t dt \tag{13}$$

where,

- OF_I : ITAEs of frequency deviations;
- OF_{II} : ITAEs of area control errors;
- OF_{III} : ITAE of tie-line power deviation;
- T_{st} : Total simulation time.

These sub-objectives are provided weights depending on their importance and a single objective function is developed combining all three weighted sub-objectives. The structure of developed objective function is given as

$$OF = (O_1)(OF_I) + (O_2)(OF_{II}) + (O_3)(OF_{III}) \tag{14}$$

where, O_1, O_2 and O_3 are weights of OF_I, OF_{II} and OF_{III} , respectively.

Implementation of FAHP method for AGC problem

In this contribution, for determining the weights associated with sub-objective functions, FAHP method is implemented, following the steps priorly discussed in Sect. “Fuzzy analytic hierarchy process”. The sub-objectives (11), (12) and (13) are signified with highest, higher and above average significance level, respectively. Corresponding to these significance levels, the weights are calculated using FAHP method discussed in Sect. “Fuzzy analytic hierarchy process”. Here, the sub-objectives OF_I, OF_{II} and OF_{III} are considered as attributes as well as alternatives. Therefore, the value of M and N will be same, i.e 3, for this problem. The significance level of one sub-objective with respect to other, is assigned as follows: (Table 6)

- OF_I is at “Highest” significance level with respect to OF_{III} .
- OF_I is at “Higher” significance level with respect to OF_{II} .
- OF_{II} is at “Above average” significance level with respect to OF_{III} .

Considering these significance levels, Table 1 is further transformed to Table 7. Corresponding to the fuzzy elements presented in Table 7 and referring to (2), (15) is generated.

$$A = \begin{matrix} & OF_1 & OF_2 & OF_3 \\ \begin{matrix} OF_1 \\ OF_2 \\ OF_3 \end{matrix} & \begin{bmatrix} (1, 1, 1) & (7, 8, 9) & (8, 9, 10) \\ (\frac{1}{7}, \frac{1}{8}, \frac{1}{9}) & (1, 1, 1) & (5, 6, 7) \\ (\frac{1}{8}, \frac{1}{9}, \frac{1}{10}) & (\frac{1}{5}, \frac{1}{6}, \frac{1}{7}) & (1, 1, 1) \end{bmatrix} \end{matrix} \tag{15}$$

By exploiting (3), geometric means (GM_i) are calculated using as

$$\begin{aligned} GM_1 &= [1 \times 9 \times 10]^{1/3} = 4.4814 \\ GM_2 &= [1/9 \times 1 \times 7]^{1/3} = 0.9196 \\ GM_3 &= [1/10 \times 1/7 \times 1]^{1/3} = 0.2426 \end{aligned} \quad (16)$$

The cumulative geometric mean is determined as

$$\sum_{i=1}^N GM_i = 4.4814 + 0.9196 + 0.2426 = 5.6437 \quad (17)$$

The fuzzy weights FO_{U1} , FO_{U2} and FO_{U3} , are calculated with the help of (4) by utilizing the values from (16) and (17) as

$$\begin{aligned} FO_{U1} &= 0.7633 \\ FO_{U2} &= 0.1783 \\ FO_{U3} &= 0.0583 \end{aligned} \quad (18)$$

The values of fuzzy weights obtained in (18) are calculated by taking upper range values into consideration. Similarly lower and middle range values are calculated which are presented in (19) and (20), respectively.

$$\begin{aligned} FO_{L1} &= 0.7941 \\ FO_{L2} &= 0.1630 \\ FO_{L3} &= 0.0430 \end{aligned} \quad (19)$$

$$\begin{aligned} FO_{M1} &= 0.7800 \\ FO_{M2} &= 0.1704 \\ FO_{M3} &= 0.0496 \end{aligned} \quad (20)$$

The calculation of best non-fuzzy performance (BNFP) value as weight is done by utilizing (5)

$$\begin{aligned} O_1 &= 0.7791 \\ O_2 &= 0.1706 \\ O_3 &= 0.0503 \end{aligned} \quad (21)$$

Substituting these weights in overall objective function, (14) can be updated as follows:

$$OF = 0.7791(OF_I) + 0.1706(OF_{II}) + 0.0503(OF_{III}) \quad (22)$$

By putting values of OF_I , OF_{II} and OF_{III} from (11), (12) and (13), respectively, in (22), it is further modified to:

$$OF = 0.7791 \left(\int_0^{T_{st}} \Delta f_I t dt + \int_0^{T_{st}} \Delta f_{II} t dt \right) + 0.1706 \left(\int_0^{T_{st}} ACE_I t dt + \int_0^{T_{st}} ACE_{II} t dt \right) + 0.0503 \left(\int_0^{T_{st}} \Delta Z_{tie-line} t dt \right) \quad (23)$$

In order to optimize (23), it becomes necessary to define its boundary constraints. The subjected boundary constraints are defined as follows:

$$\begin{aligned} \Gamma_P^{min} &< \Gamma_P < \Gamma_P^{max} \\ \Gamma_I^{min} &< \Gamma_I < \Gamma_I^{max} \\ \Gamma_D^{min} &< \Gamma_D < \Gamma_D^{max} \\ F^{min} &< F < F^{max} \end{aligned} \quad (24)$$

To optimize objective function (23), subjected to constraints shown in (24), Jaya algorithm is implemented, which is discussed further in Sect. “[Jaya optimization algorithm](#)”.

Jaya optimization algorithm

The Jaya optimization algorithm (JOA) is inspired by the Sanskrit word of “victory”, represented as “Jaya”. It was first developed to solve both constrained and unconstrained optimization problems^{37,38}. By eliminating less effective solutions, solutions within the Jaya population tend to converge towards the global optimum, mirroring the concept of “survival of the fittest” found in nature. Interestingly, this algorithm relies only on the total number of iterations and the size of the population. It does not require any particular controlling parameters.

The basic structure of working of JOA can be described in the below-mentioned five phases:

1. **Initialization** The process is started by initializing a set of population comprising of candidate solutions. Usually, these solutions are shown as vectors in the optimization problem’s search space.
2. **Determination** Utilizing the optimization problem’s objective function, determine candidate solution. Each solution is assigned with a fitness value by the objective function. This fitness value evaluates performance of the candidate corresponding to problem.

Fuzzy	Fuzzy element as a	Significance
Performance index	TFM function	Level
9	(8,9,10)	Highest
8	(7,8,9)	Higher
6	(5,6,7)	Above average
1	(1,1,1)	Identical

Table 7. Performance indices with TFM function and their relative significance.

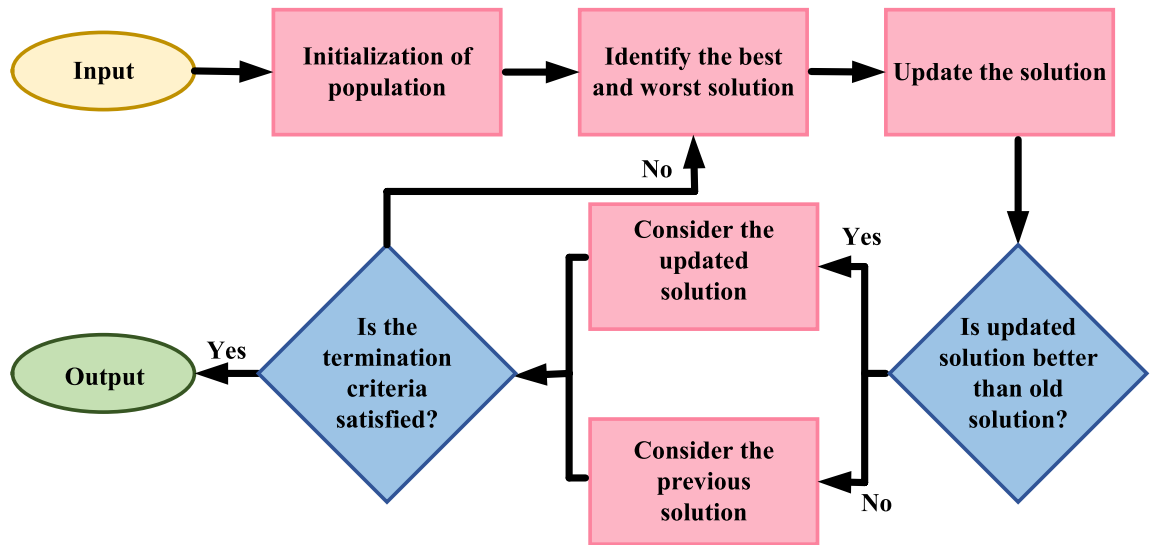


Figure 2. Jaya optimization.

3. *Regeneration* For each iteration, the candidate solution is regenerated such that it moves towards the best solution (solution having lowest fitness value), ignoring the worst solution (solution having highest fitness value).
4. *Discontinuation* Once the predetermined number of iterations is completed or termination criterion is satisfied, the process is discontinued.
5. *Final solution* The solution obtained just before discontinuing the process is termed as the final solution.

The flowchart for JOA is provided in Fig. 2. In JOA, the expression for updated solution is represented as follows:

$$\mathcal{O}_{x,y}^i = \mathcal{O}_{x,y}^i + \mathcal{O}_1 + \mathcal{O}_2 \tag{25}$$

where,

$$\left. \begin{aligned} \mathcal{O}_1 &= \alpha_1(\mathcal{O}_{best,b}^i - \mathcal{O}_{x,y}^i) \\ \mathcal{O}_2 &= -\alpha_2(\mathcal{O}_{worst,b}^i - \mathcal{O}_{x,y}^i) \end{aligned} \right\} \tag{26}$$

In (25), $\mathcal{O}_{x,y}^i$ and $\mathcal{O}_{x,y}^i$ are updated solution and current solution respectively, for x^{th} candidate and y^{th} decision parameter. While, $\mathcal{O}_{best,y}^i$ and $\mathcal{O}_{worst,y}^i$ in (26) denote best and worst solution, respectively and α_1 and α_2 are random variables. An updated solution is produced after every iteration. If this revised solution performs better than the original, it will be considered for further iterations.

Results and discussions

This work is expanded on the framework developed by Ali and Abd-Elazim³⁶ by analysing a 2-APS. Table 6 outlines the constraints that control the controller parameters. However, (23) provides specifics on the overall objective function that is intended to be minimised. The boundary conditions for these controller parameters are expressed in (24). Table 8 details the step load disturbance assigned to each area in each of the six experimental cases that are investigated to thoroughly evaluate the effectiveness of the FAHP method-assisted PID controller.

The numerical data obtained after performing the simulations for experimental cases I to VI are provided in Tables 9, 10, 11, 12, 13 and 14, respectively, for analytical discussion. Each table provides the most fitted values of objective function (OF), sub-objective functions (OF_I , OF_{II} and OF_{III}), and controller parameters (Γ_P , Γ_I , Γ_D and F), obtained by implementing JOA, SCA, LJA, NMSA, SOSA and EHOA, for the corresponding experimental case. Along with these, the settling time and peak overshoot values of responses (Fig. 3– 20)

Step load deviations		
Experimental cases	Area 1	Area 2
I	0.032	0
II	0	0.032
III	0.032	0.032
IV	0.032	-0.032
V	0.032	0.064
VI	0.064	0.032

Table 8. Step load deviations.

		JOA	SCA	LJA	NMSA	SOSA	EHOA
Fitness	OF	0.01770	0.03335	0.02262	0.04087	0.02609	0.02641
	OF_I	0.02044	0.03879	0.02605	0.04716	0.03027	0.03066
	OF_{II}	0.00536	0.00942	0.00762	0.01296	0.00799	0.00803
	OF_{III}	0.00879	0.01561	0.01139	0.02035	0.01231	0.01244
Decision parameters	Γ_P	1.88711	1.76927	2.87765	2.13089	2.15094	2.22966
	Γ_I	2.98252	2.49641	2.87080	2.00521	2.67468	2.72156
	Γ_D	0.52462	1.15719	1.14092	1.24554	1.12535	1.20696
	F	356.830	433.202	273.225	177.700	347.199	349.361
Settling time (s)	Δf_I	2.21656	4.16017	2.25456	2.99855	3.51192	3.63688
	Δf_{II}	3.23523	5.00380	4.36233	4.89006	3.46292	3.48560
	$\Delta Z_{tie-line}$	3.14423	5.41283	4.49587	4.99221	3.64359	3.65955
Peak overshoots (p.u.)	Δf_I	0.03119	0.02229	0.02180	0.02155	0.02238	0.02156
	Δf_{II}	0.01626	0.00998	0.00900	0.00906	0.00973	0.00913
	$\Delta Z_{tie-line}$	0.00541	0.00377	0.00314	0.00356	0.00351	0.00334

Table 9. Results for case analysis I.

indicating frequency deviation in area 1 and area 2, and tie-line power deviation, for corresponding experimental cases, are also tabulated in each table.

The outcomes of experimental cases I and II are tabulated in Tables 9 and 10, respectively. The least value (i.e. optimum value) of OF_I , OF_{II} , OF_{III} and OF is achieved by JOA, followed by LJA, for both cases. For case I and case II, the responses for frequency deviation in area 1 is shown in Fig. 3 and 6, respectively, and the responses for frequency deviation in area 2 are shown in Fig. 4 and 7, respectively. It can be seen from the responses that, for both cases, the response shown by JOA settles faster than the other algorithms. Similar outcomes is seen for tie-line deviation of case I (Fig. 5) and case II (Fig. 8). The exact settling time values can be seen in Table 9 and Table 10. So, for case I and case II, JOA is proved most efficient among all the considered algorithms.

Tables 11 and 12 provide a summary of the outcomes of experimental cases III and IV, respectively. In both situations, JOA showcased lowest (i.e., optimal) values for OF_I , OF_{II} , OF_{III} , and OF , followed by LJ algorithm in case III and EHO algorithm in case IV. The frequency deviation responses for area 1 in cases III and IV are shown in Fig(s). 9 and 12, respectively, and those for area 2 are shown in Fig(s). 10 and 13. These responses clearly show that the JOA settles more quickly than other algorithms in both scenarios. The tie-line deviation responses for cases III (Fig. 11) and IV (Fig. 14) show a similar trend. Table 11 and Table 12 tabulated their specific settling time values. From the discussion, it is clear that JOA outperformed all the other algorithms for case III and case IV.

The results of experimental cases V and VI are outlined in Tables 13 and 14, respectively. The optimal values for OF_I , OF_{II} , OF_{III} , and OF are displayed by the JOA in both cases. In case V, the NMS algorithm came in second, and in case VI, the SOSA algorithm performed better after JOA. Fig(s). 15 and 18, respectively, display the frequency deviation responses for area 1 in cases V and VI, while Fig(s). 16 and 18 display the responses for area 2. These plots conclusively show that in both scenarios, the JOA settles earlier than alternative algorithms. An analogous pattern can be seen in the tie-line deviation responses for cases V (Fig. 17) and VI (Fig. 20). Tables 13 and 14 tabulated the values of their respective settling times. Similar to all the above cases, even for these cases, JOA performed the best among all the algorithms.

A statistical analysis is provided in Table 15. This table tabulates mean (OF_{Mean}), minimum (OF_{Min}), maximum (OF_{Max}) and standard deviation (OF_{SD}) values of objective function (OF) obtained from JOA, SCA, LJA, NMSA, SOSA and EHOA, for all six cases. From Table 15, it is observed that, JOA is providing the lowest values for OF_{Mean} , OF_{Min} , OF_{Max} and OF_{SD} for all six cases. The outcome performance of other algorithms vary throughout all the six cases, while JOA is seen being consistent by maintaining the least OF_{Mean} , OF_{Min} , OF_{Max} and OF_{SD} values for case I to case VI.

		JOA	SCA	LJA	NMSA	SOSA	EHOA
Fitness	OF	0.01731	0.03335	0.02262	0.04086	0.02609	0.02641
	OF_I	0.01996	0.03879	0.02605	0.04715	0.03028	0.03066
	OF_{II}	0.00575	0.00942	0.00762	0.01296	0.00799	0.00803
	OF_{III}	0.00858	0.01561	0.01139	0.02035	0.01231	0.01244
Decision parameters	Γ_P	2.16060	1.76927	2.87765	2.13089	2.15094	2.22966
	Γ_I	2.99912	2.49641	2.87080	2.00521	2.67468	2.72156
	Γ_D	0.64784	1.15719	1.14092	1.24554	1.12535	1.20696
	F	470.811	433.202	273.225	177.700	347.199	349.361
Settling time (s)	Δf_I	3.29438	5.00379	4.36268	4.88837	3.46291	3.48559
	Δf_{II}	1.96761	4.15989	2.25635	2.99978	3.51762	3.64273
	$\Delta Z_{tie-line}$	3.44820	5.41284	4.49579	4.99238	3.64359	3.65957
Peak overshoots (p.u.)	Δf_I	0.01402	0.00998	0.00900	0.00906	0.00973	0.00913
	Δf_{II}	0.02841	0.02229	0.02180	0.02155	0.02238	0.02156
	$\Delta Z_{tie-line}$	0.00471	0.00377	0.00314	0.00356	0.00351	0.00334

Table 10. Results for case analysis II.

		JOA	SCA	LJA	NMSA	SOSA	EHOA
Fitness	OF	0.02541	0.06769	0.03822	0.05151	0.05128	0.04371
	OF_I	0.02984	0.07949	0.04488	0.06048	0.06022	0.05132
	OF_{II}	0.00000	0.00000	0.00000	0.00000	0.00000	0.00000
	OF_{III}	0.01268	0.03378	0.01908	0.02571	0.02559	0.02181
Decision parameters	Γ_P	2.16060	1.76927	2.87765	2.13089	2.15094	2.22966
	Γ_I	2.95342	2.77400	2.61036	2.29569	2.54692	2.89826
	Γ_D	0.52539	0.93834	0.78534	0.87023	1.24136	1.23978
	F	260.322	275.477	351.305	228.395	365.123	490.703
Settling time (s)	Δf_I	2.17045	4.03241	2.35049	2.67387	3.26389	3.85170
	Δf_{II}	2.17045	4.03241	2.35049	2.67387	3.26389	3.85170
	$\Delta Z_{tie-line}$	0.00000	0.00000	0.00000	0.00000	0.00000	0.00000
Peak overshoots (p.u.)	Δf_I	0.03532	0.02857	0.03006	0.02894	0.02296	0.02298
	Δf_{II}	0.03532	0.02857	0.03006	0.02894	0.02296	0.02298
	$\Delta Z_{tie-line}$	0.00000	0.00000	0.00000	0.00000	0.00000	0.00000

Table 11. Results for case analysis III.

		JOA	SCA	LJA	NMSA	SOSA	EHOA
Fitness	OF	0.02403	0.03794	0.02752	0.03111	0.02888	0.02533
	OF_I	0.02609	0.03723	0.02890	0.03188	0.03016	0.02672
	OF_{II}	0.01302	0.02839	0.01627	0.02018	0.01783	0.01524
	OF_{III}	0.01788	0.04398	0.02452	0.03079	0.02628	0.02192
Decision parameters	Γ_P	2.46482	2.34051	2.54515	2.47623	2.32523	2.54709
	Γ_I	2.98858	1.94360	2.94214	2.52240	2.57513	2.835346
	Γ_D	1.00376	0.84323	1.57115	1.58464	1.28716	1.25174
	F	398.739	467.817	379.625	205.922	369.009	469.840
Settling time (s)	Δf_I	3.51062	4.40854	3.95176	4.33906	4.01833	3.82893
	Δf_{II}	3.51062	4.40854	3.95176	4.33906	4.01833	3.82893
	$\Delta Z_{tie-line}$	3.70408	6.00784	5.49316	4.22087	4.00612	3.93501
Peak overshoots (p.u.)	Δf_I	0.02183	0.02357	0.01773	0.01791	0.01960	0.01971
	Δf_{II}	0.02183	0.02357	0.01773	0.01791	0.01960	0.01971
	$\Delta Z_{tie-line}$	0.00715	0.00819	0.00594	0.00617	0.00652	0.00621

Table 12. Results for case analysis IV.

		JOA	SCA	LJA	NMSA	SOSA	EHOA
Fitness	OF	0.03877	0.04128	0.06272	0.07654	0.05452	0.05560
	OF_I	0.04515	0.04797	0.07318	0.08939	0.06373	0.06498
	OF_{II}	0.00521	0.00532	0.00792	0.00878	0.00690	0.00697
	OF_{III}	0.01951	0.02134	0.03110	0.03780	0.02649	0.02712
Decision parameters	Γ_P	1.62401	1.59717	1.63668	2.67985	1.93025	2.06716
	Γ_I	2.92798	2.88402	2.32600	2.63987	2.68320	2.72282
	Γ_D	0.48128	0.43335	0.48760	1.32552	0.76239	0.82656
	F	355.622	218.227	369.819	440.721	300.932	228.823
Settling time (s)	Δf_I	2.38233	2.45129	3.36826	3.97366	2.87172	3.01707
	Δf_{II}	2.10890	2.16707	2.53177	3.18600	2.18507	2.23903
	$\Delta Z_{tie-line}$	3.05619	3.18510	3.68247	4.47757	3.46559	3.58744
Peak overshoots (p.u.)	Δf_I	0.04554	0.04734	0.04591	0.02496	0.03652	0.03449
	Δf_{II}	0.06934	0.07210	0.06923	0.04199	0.05680	0.05451
	$\Delta Z_{tie-line}$	0.00587	0.00616	0.00592	0.00302	0.00453	0.00424

Table 13. Results for case analysis V.

		JOA	SCA	LJA	NMSA	SOSA	EHOA
Fitness	OF	0.04058	0.08797	0.08657	0.07043	0.08278	0.09451
	OF_I	0.04739	0.10230	0.10111	0.08229	0.09664	0.11049
	OF_{II}	0.00555	0.00996	0.00964	0.00846	0.00971	0.00957
	OF_{III}	0.01980	0.04555	0.04285	0.03453	0.04107	0.04659
Decision parameters	Γ_P	1.81290	2.02888	2.94046	1.97933	1.86144	2.79796
	Γ_I	2.90251	2.26469	2.60156	2.44598	2.17972	2.98638
	Γ_D	0.53182	0.33129	1.57187	0.91227	0.51777	2.14128
	F	199.643	256.339	269.611	433.240	393.858	410.815
Settling time (s)	Δf_I	1.64124	3.88906	3.59934	2.55364	3.02945	5.43786
	Δf_{II}	2.46416	4.49774	4.40004	3.28118	4.06844	6.06677
	$\Delta Z_{tie-line}$	3.13768	5.30282	4.86206	3.85088	4.41652	6.56501
Peak overshoots (p.u.)	Δf_I	0.06616	0.07505	0.03835	0.05207	0.06662	0.03223
	Δf_{II}	0.04276	0.04817	0.02229	0.03351	0.04349	0.02036
	$\Delta Z_{tie-line}$	0.00546	0.00632	0.00284	0.00409	0.00556	0.00266

Table 14. Results for case analysis VI.

For further clarification of efficacy and accuracy of the outcomes obtained, Friedman rank test is carried out for JOA, SCA, LJA, NMSA, SOSA and EHOA. This test provides a non-parametric analysis, by allocating a mean rank to all of the six algorithms, and a overall Q value and p value. The outcomes are said to be verified when Q value is positive and p value is lesser than 5%. The algorithm attaining the mean rank 1 is considered to be the best among all the algorithms. Table 16 tabulates the results of Friedman rank test. The mean ranks for JOA, SCA, LJA, NMSA, SOSA and EHOA are 1, 4.83333, 3, 5, 3.33333 and 3.83333, respectively. This shows that JOA yields best performance, followed by LJA, SOSA, EHOA, SCA and NMSA. The Q value came out to be 18.28571, which is a positive value, and p value is 0.002609 which is significantly lesser than 5%. Hence these results also provide the clarity on the applicability and efficacy of Jaya algorithm.

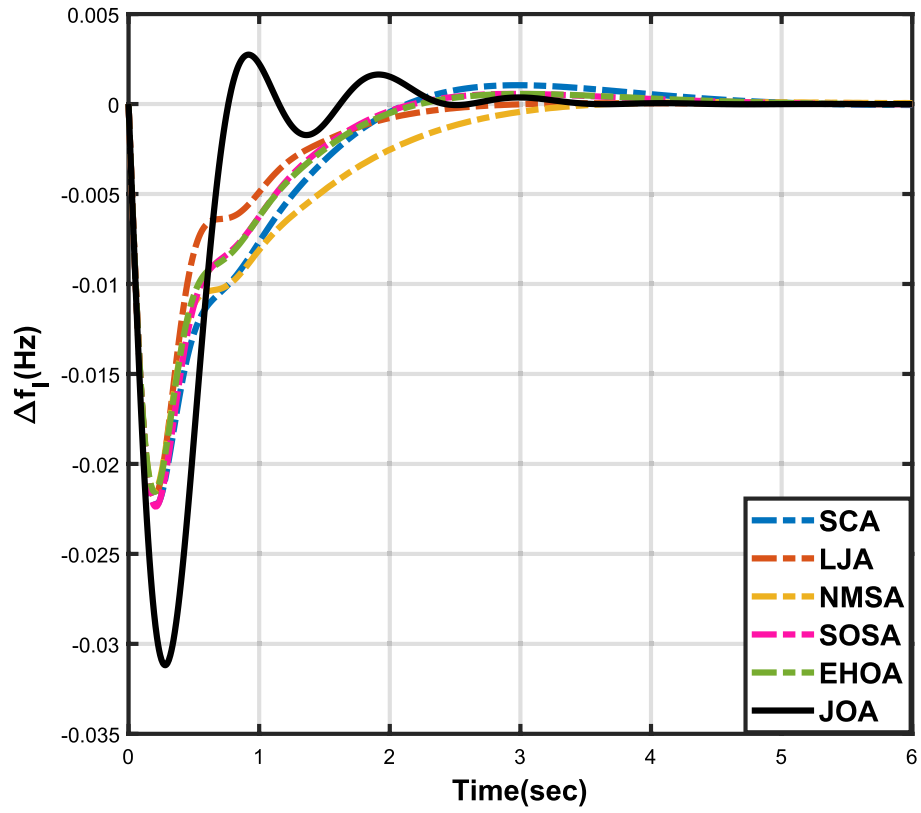


Figure 3. Case 1: Frequency fluctuations for area-1.

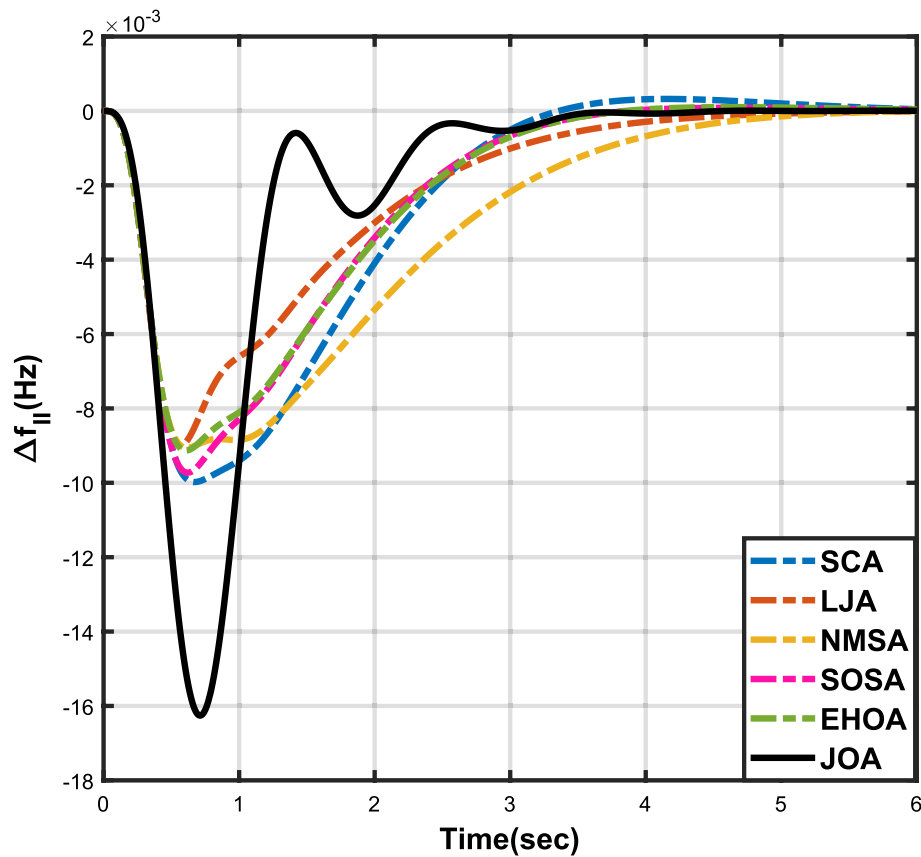


Figure 4. Case 1: Frequency fluctuations for area-2.

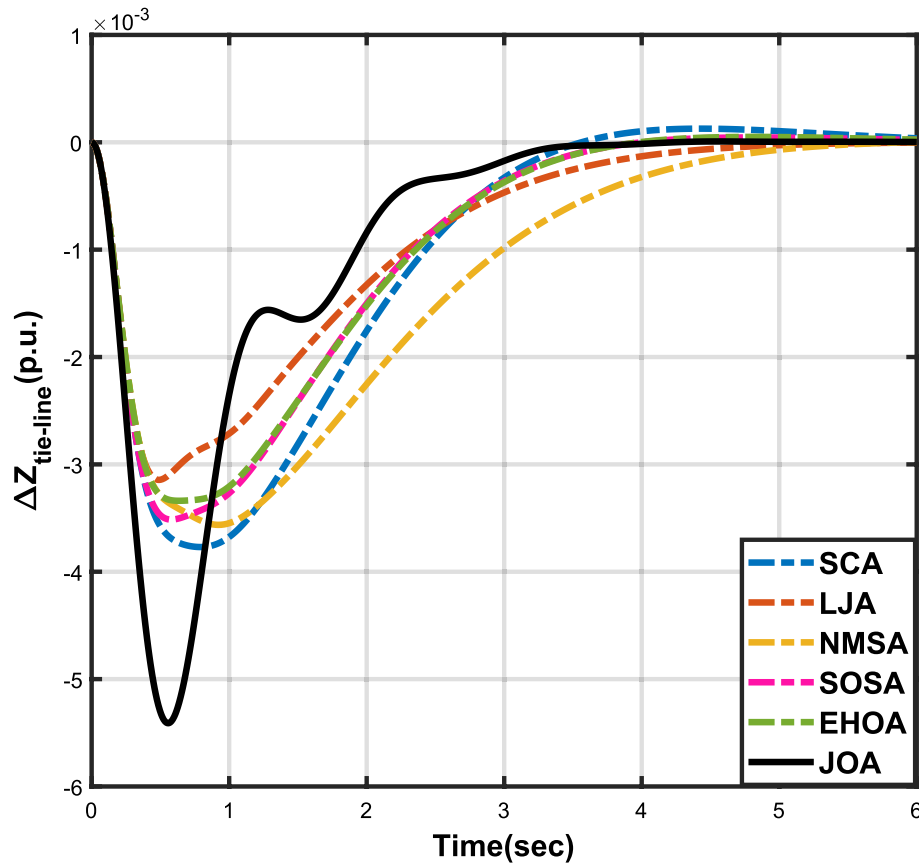


Figure 5. Case 1: Tie-line power fluctuation.

Conclusion

Assessing several attributes simultaneously, figuring out how important each factor is, and choosing a suitable method to compute the weights have always been a matter of concern for decision maker. MADM techniques have helped decision makers to deal with these concerns. One such MADM technique, i.e. FAHP technique is utilized in this contribution to determine weights corresponding to sub-objective functions. The ITAE evaluations of frequency deviations, control errors, and tie-line power deviation for AGC problem of 2-APS are taken into consideration for sub-objective functions. These sub-objective functions are employed for the design of PID controller. The objective function, constructed by combining all weighted sub-objectives, is then minimized using the JOA. The JOA's efficacy is assessed across six distinct load scenarios. Optimization is also carried out using SCA, LJA, NMSA, SOSA, and EHOA to show the efficacy of the JOA-based controller. For each of the six load variations, their results are compared, and the comparisons are shown in tabular and graphical form. Specifications like peak overshoots, settling time, decision parameters, and objective function values are compared. The outcomes showed that for all load variations taken into consideration, the JOA consistently performs better than the other algorithms. Furthermore, Friedman rank test and statistical analysis support the superiority of the JOA-based PID controller over alternative controllers.

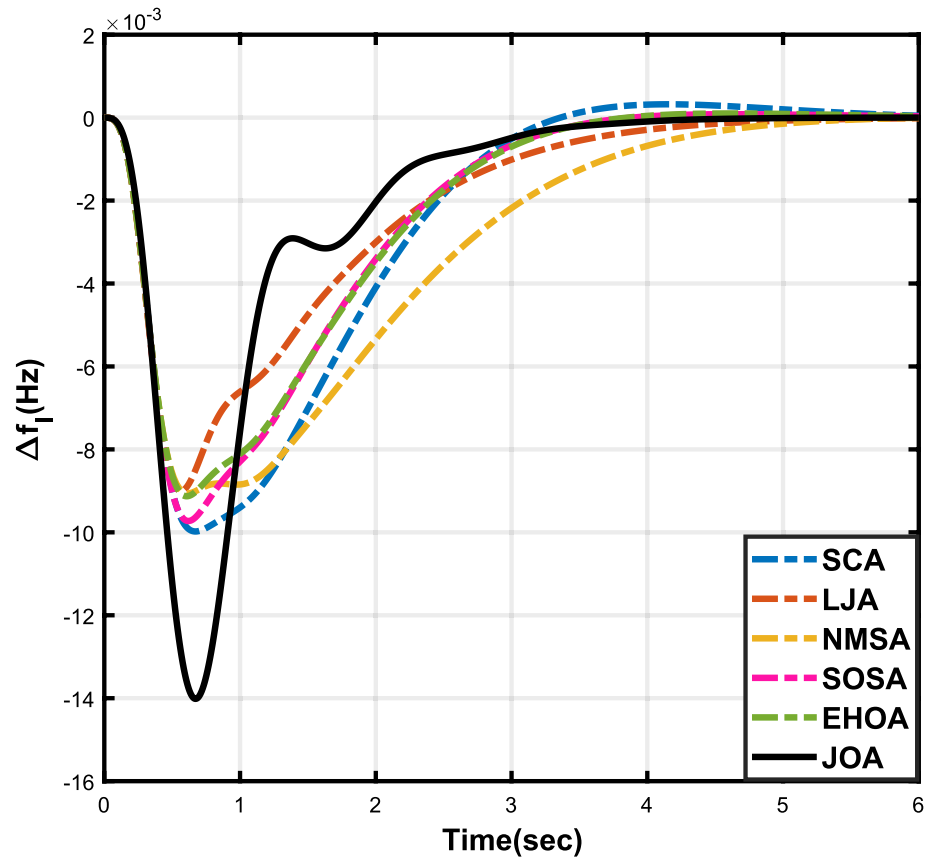


Figure 6. Case 2: Frequency fluctuations for area-1.

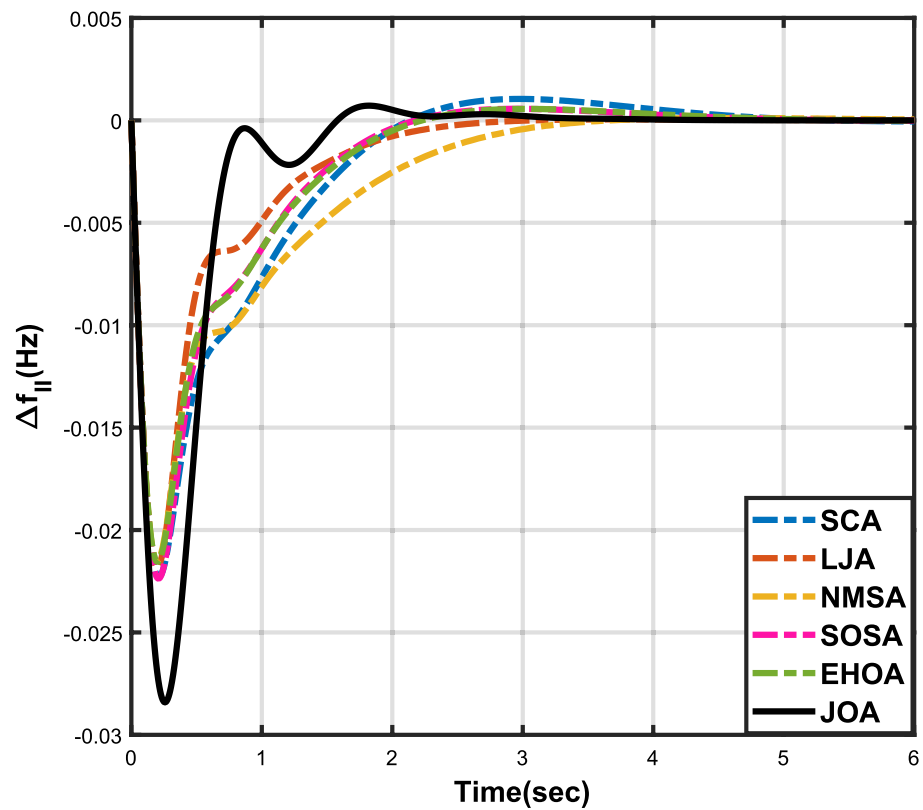


Figure 7. Case 2: Frequency fluctuations for area-2.

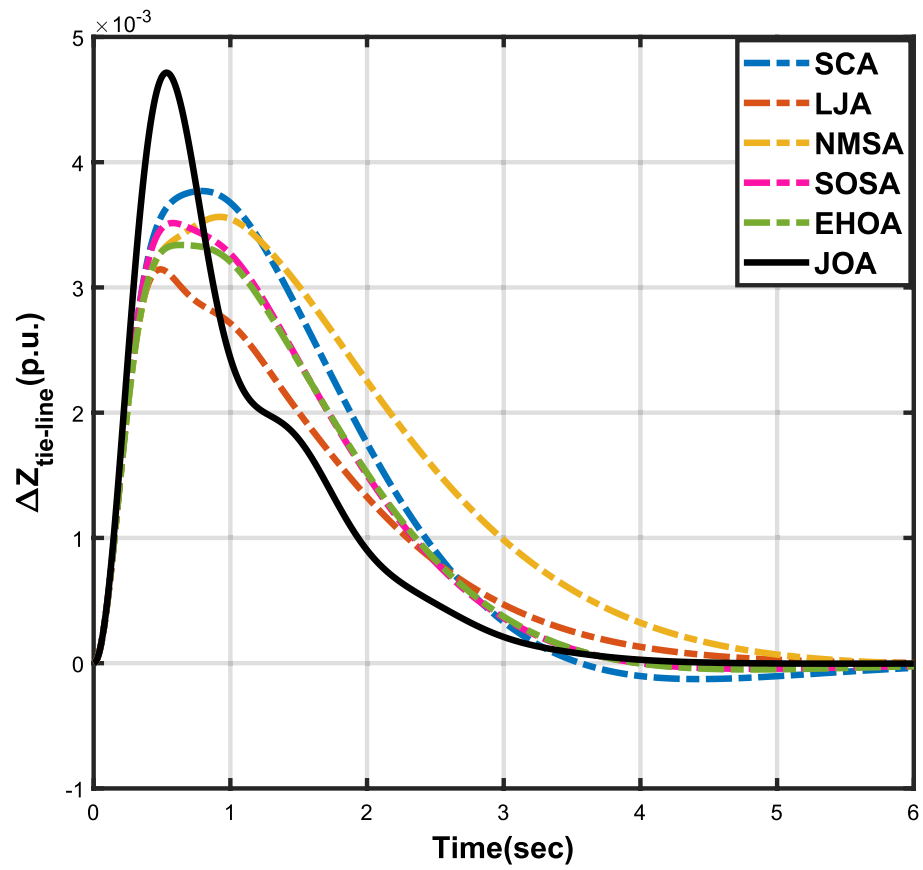


Figure 8. Case 2: Tie-line power fluctuation.

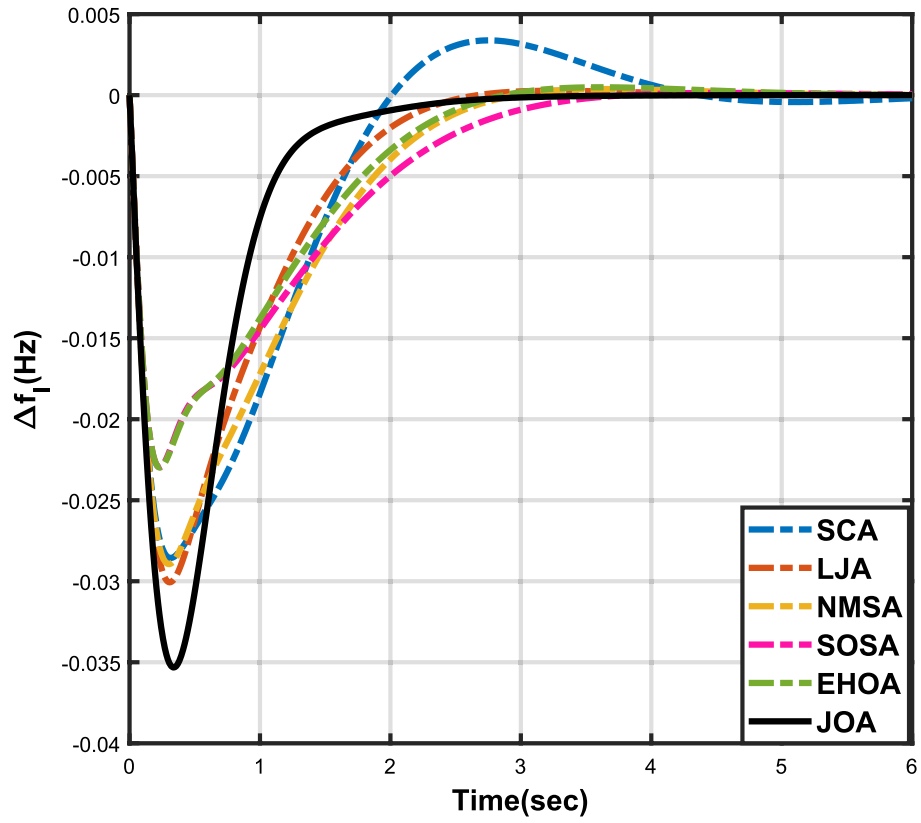


Figure 9. Case 3: Frequency fluctuations for area-1.

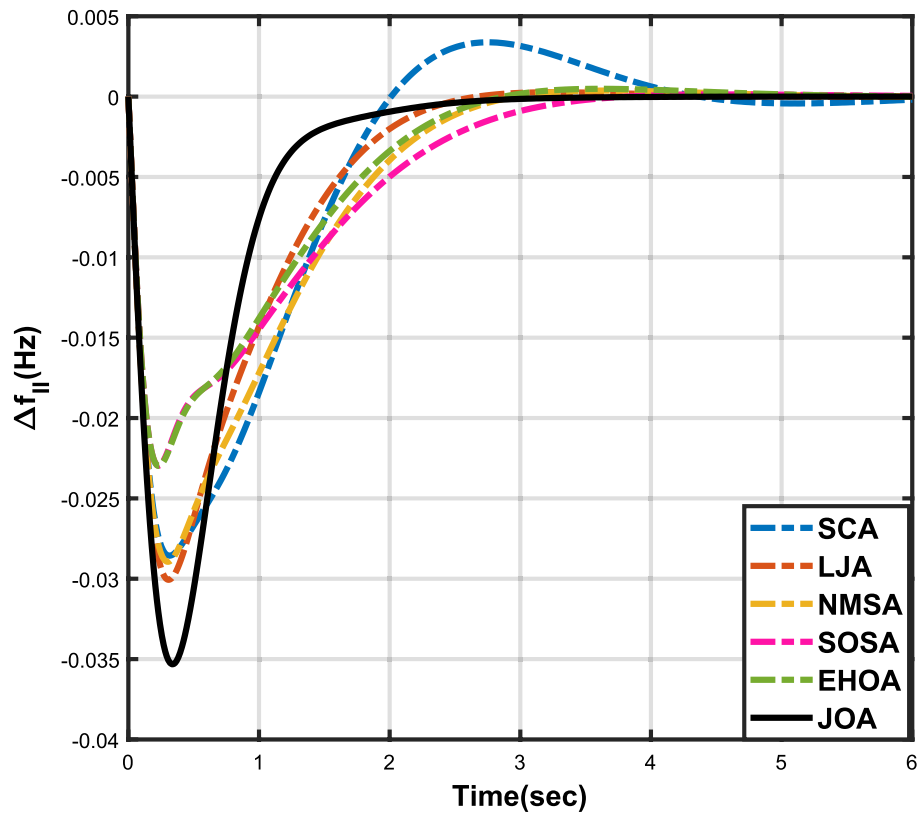


Figure 10. Case 3: Frequency fluctuations for area-2.

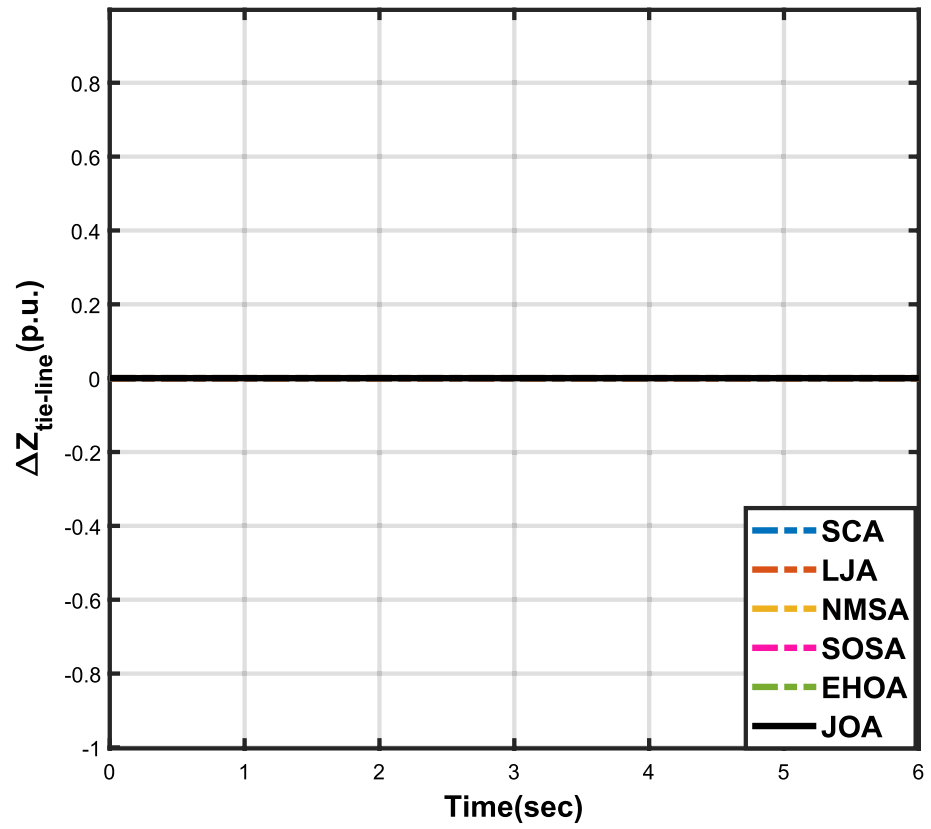


Figure 11. Case 3: Tie-line power fluctuation.

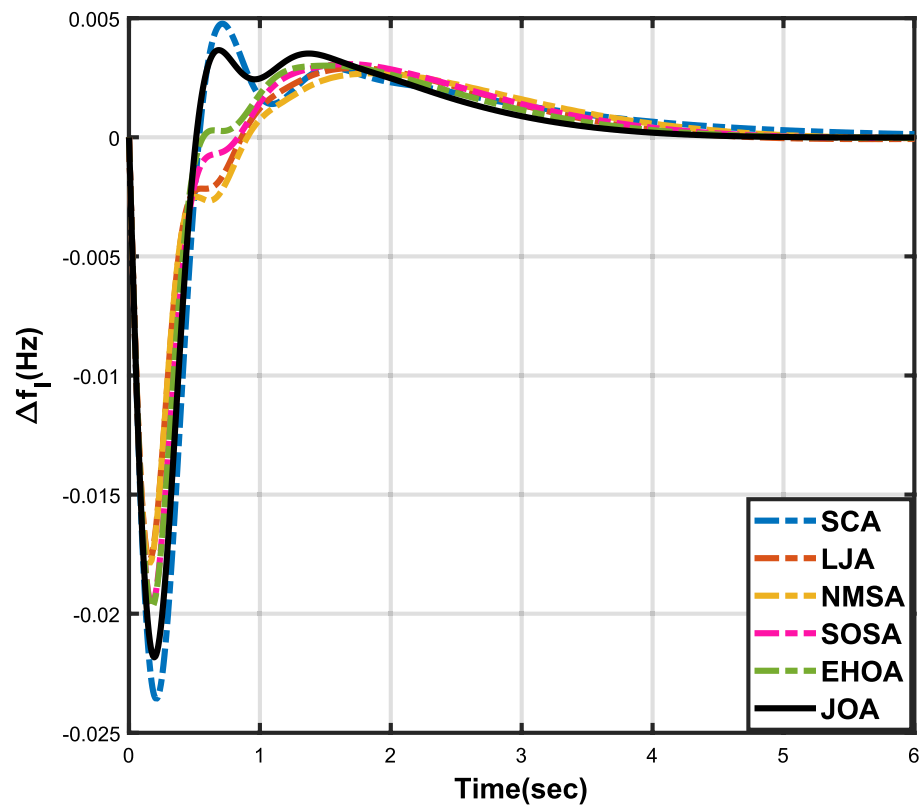


Figure 12. Case 4: Frequency fluctuations for area-1.

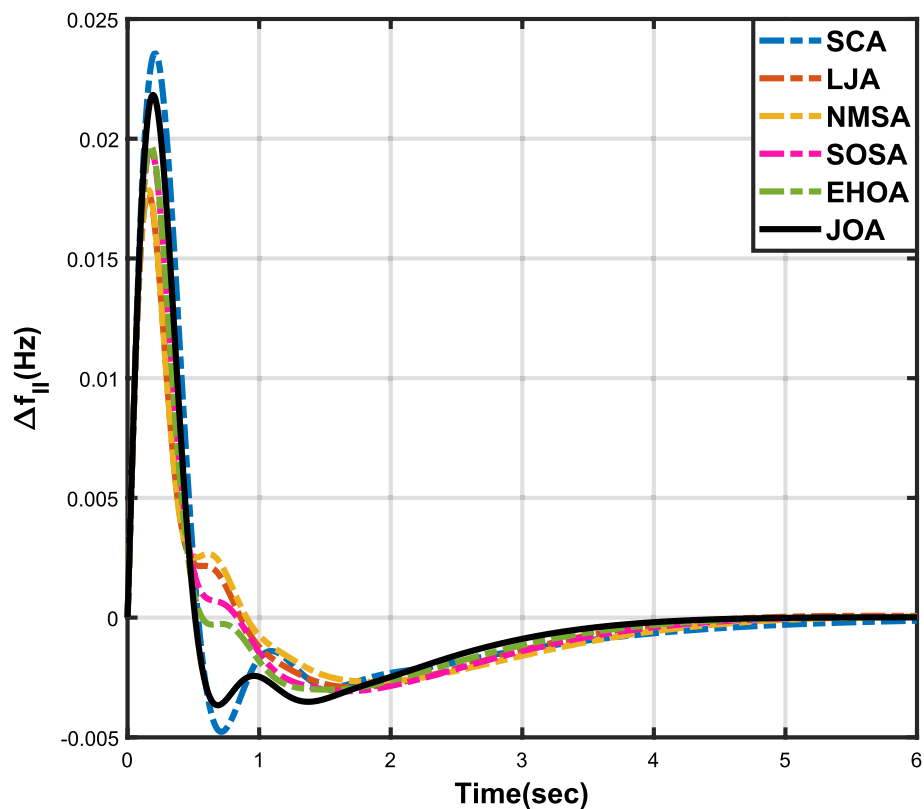


Figure 13. Case 4: Frequency fluctuations for area-2.

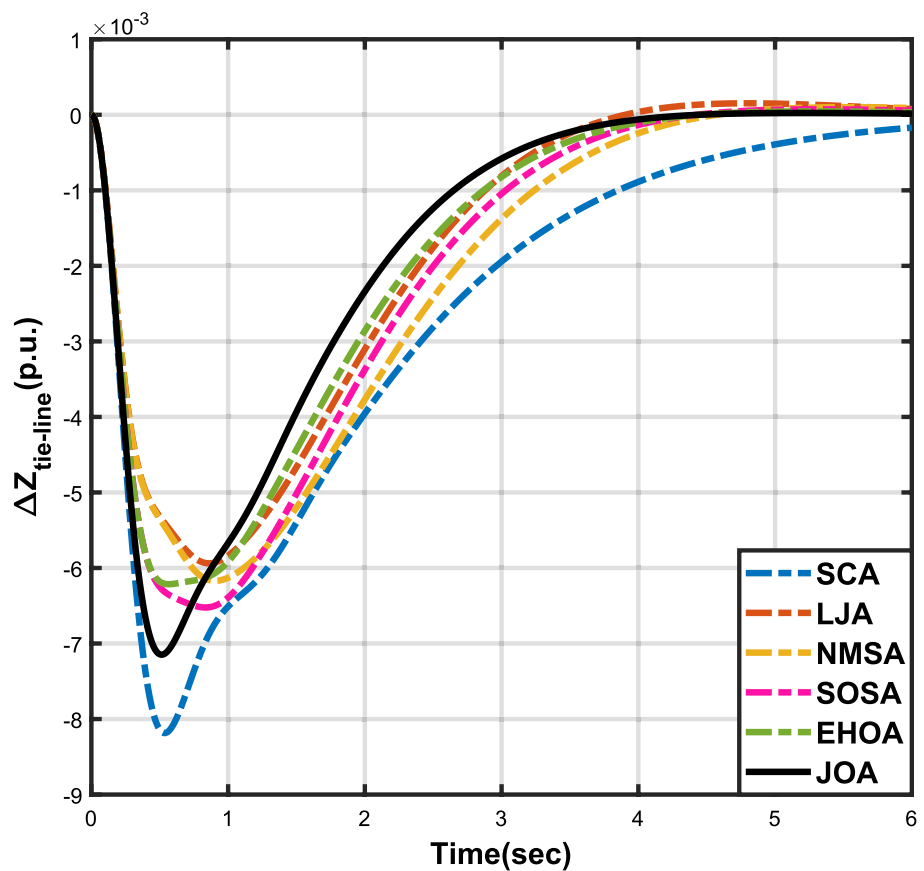


Figure 14. Case 4: Tie-line power fluctuation.

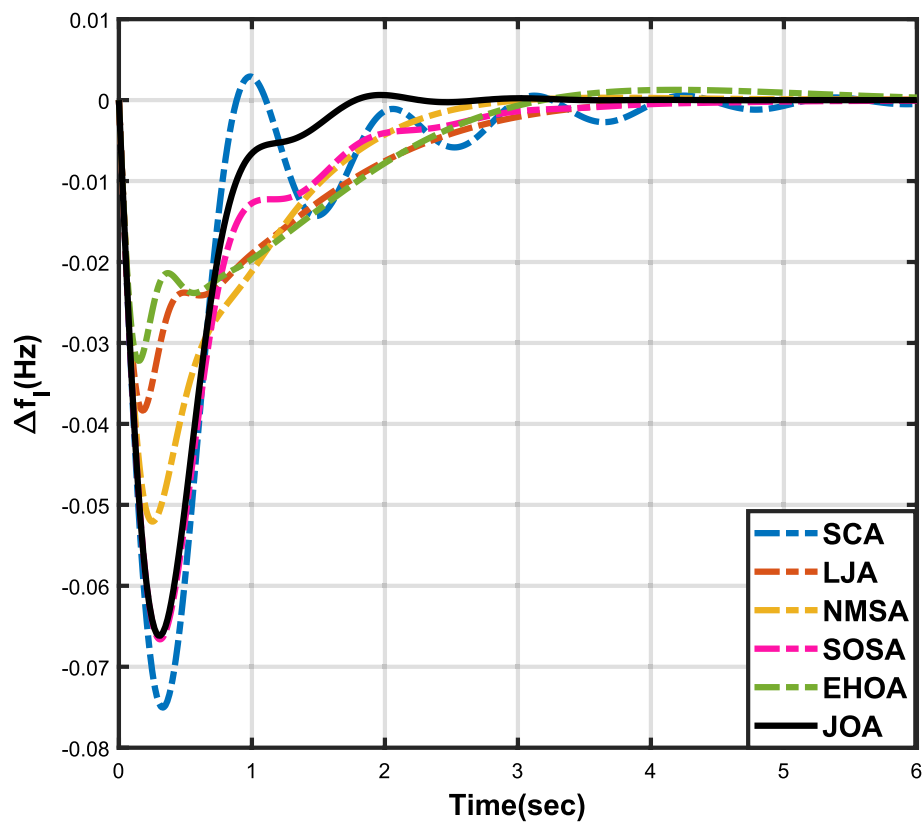


Figure 15. Case 5: Frequency fluctuations for area-1.

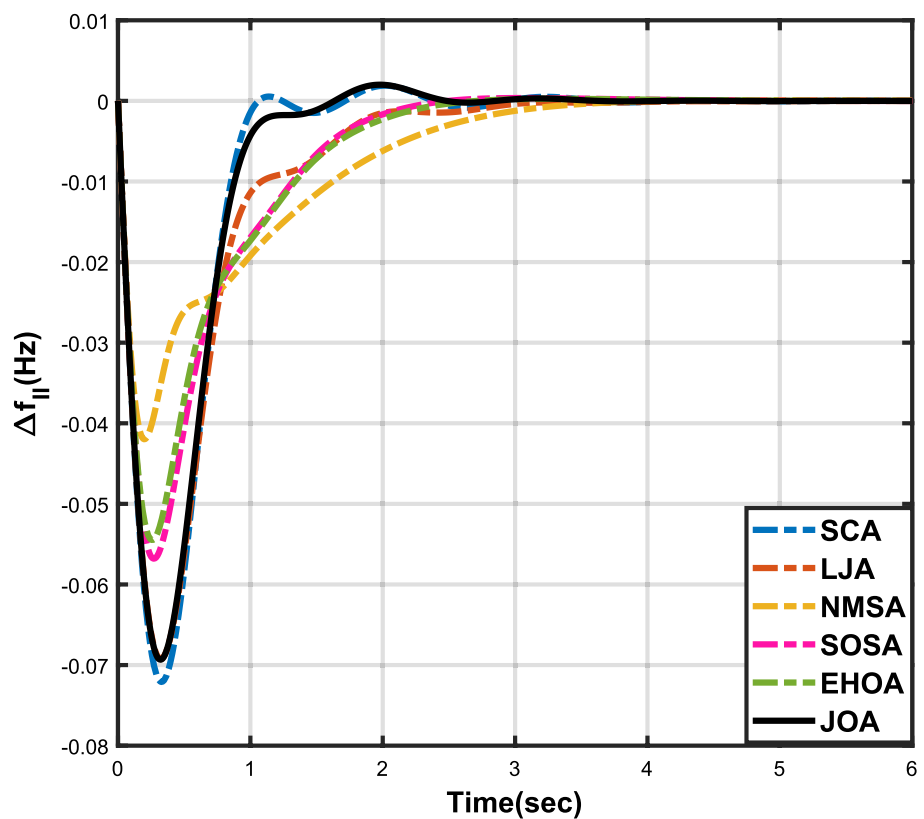


Figure 16. Case 5: Frequency fluctuations for area-2.

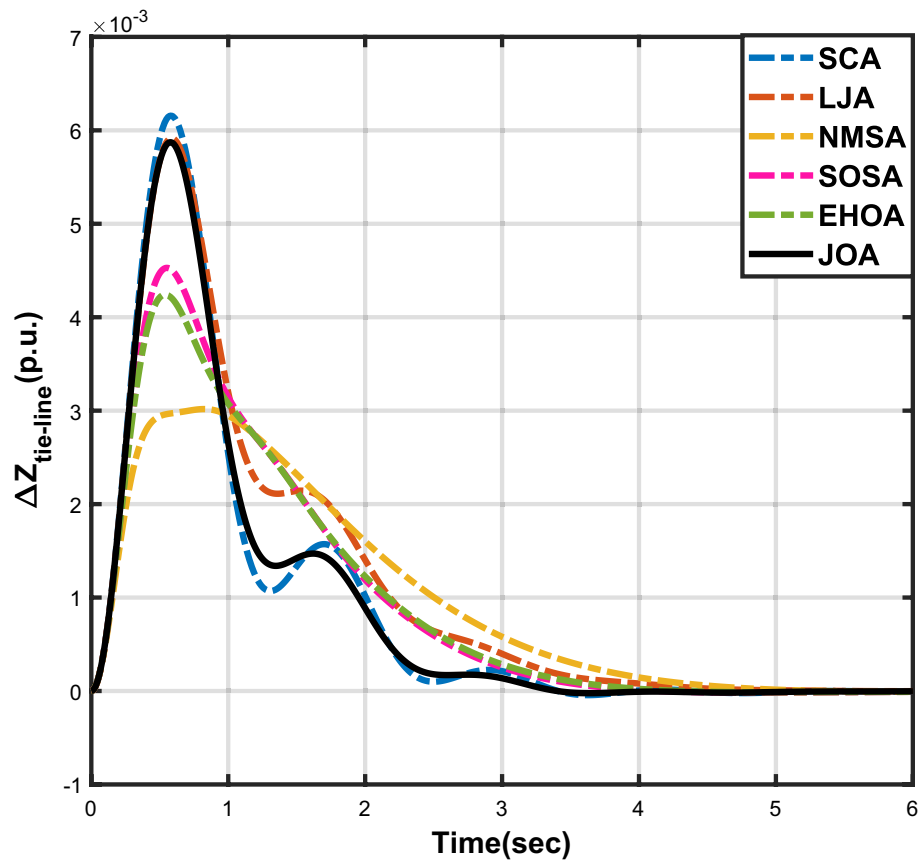


Figure 17. Case 5: Tie-line power fluctuation.

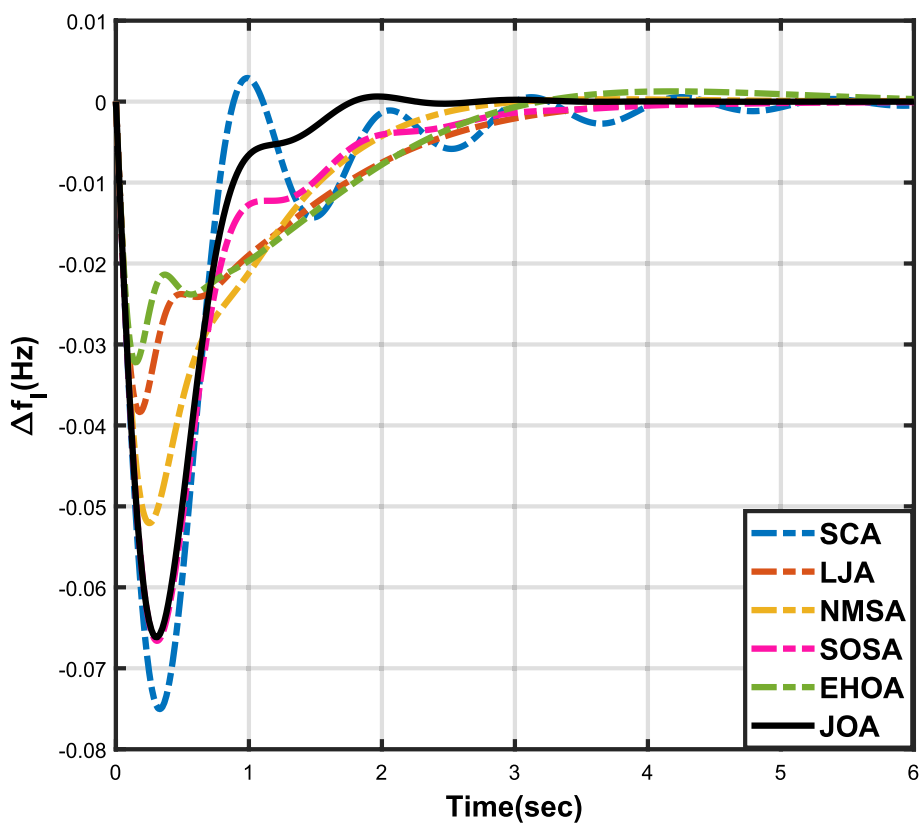


Figure 18. Case 6: Frequency fluctuations for area-1.

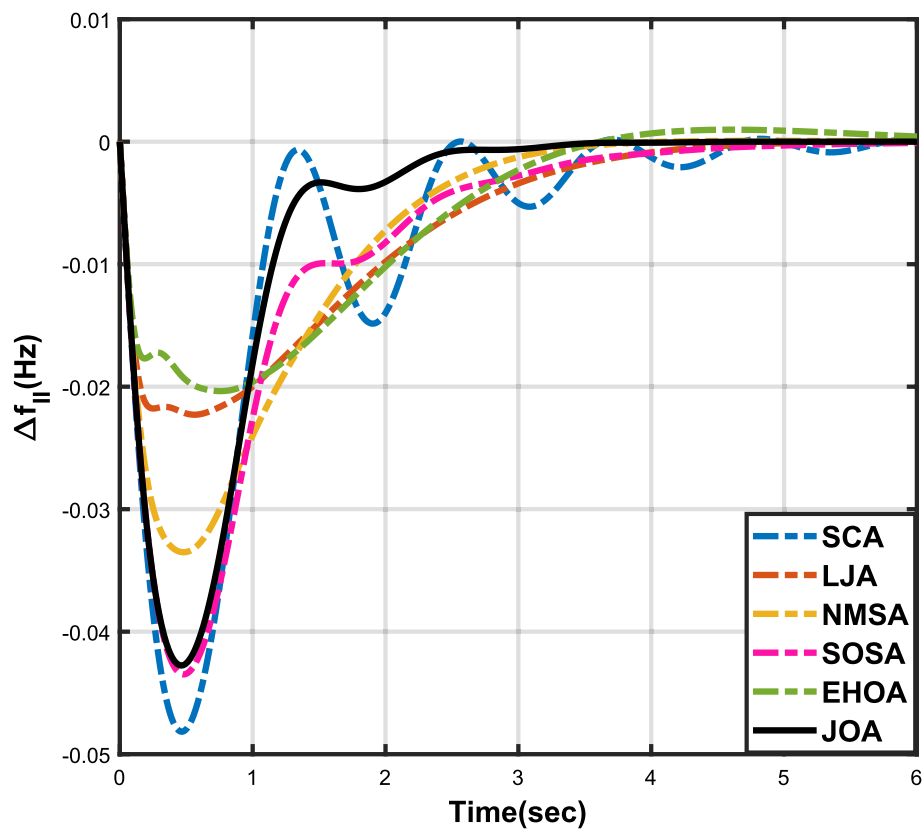


Figure 19. Case 6: Frequency fluctuations for area-2.

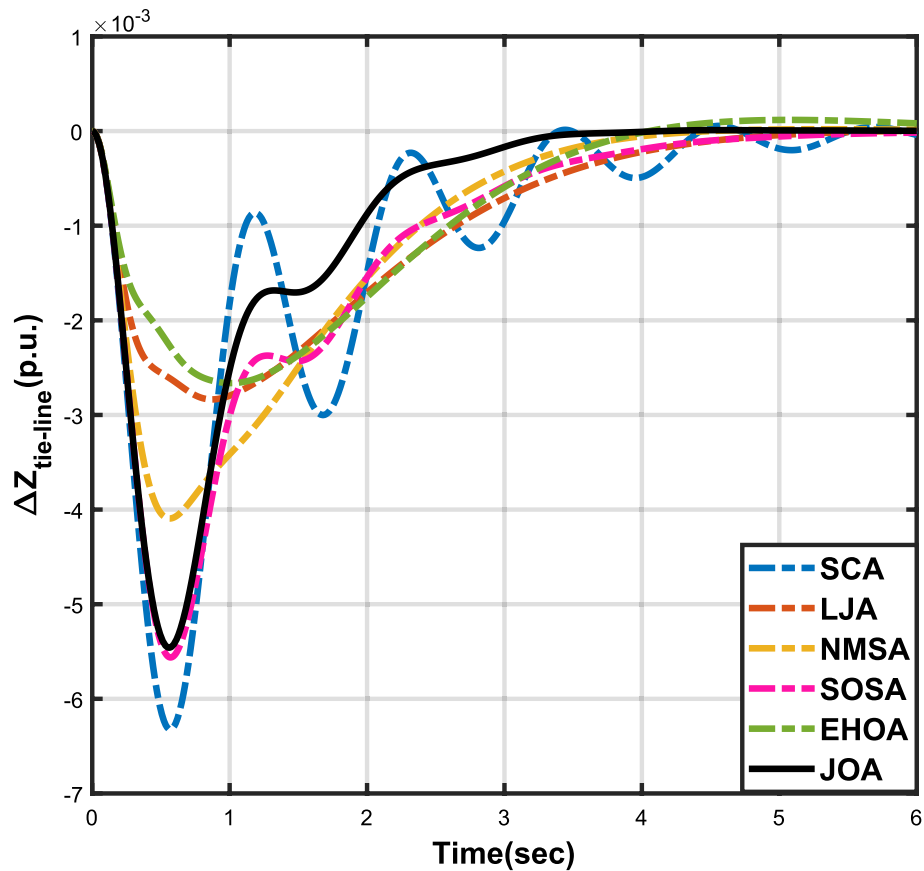


Figure 20. Case 6: Tie-line power fluctuation.

Cases	Statistical measures	JOA	SCA	LJA	NMSA	SOSA	EHOA
I	OF_{Mean}	0.01851	0.06187	0.03980	0.05172	0.02877	0.03107
	OF_{Min}	0.01770	0.03335	0.02262	0.04087	0.02609	0.02641
	OF_{Max}	0.01972	0.08366	0.06050	0.07857	0.03088	0.03842
	OF_{SD}	0.00078	0.01903	0.01637	0.01621	0.00191	0.00505
II	OF_{Mean}	0.01809	0.06187	0.03980	0.05172	0.02877	0.03107
	OF_{Min}	0.01731	0.03335	0.02262	0.04086	0.02609	0.02641
	OF_{Max}	0.02005	0.08366	0.06050	0.07857	0.03088	0.03842
	OF_{SD}	0.00112	0.01903	0.01637	0.01621	0.00191	0.00505
III	OF_{Mean}	0.03010	0.10148	0.06093	0.06738	0.05808	0.05324
	OF_{Min}	0.02541	0.06769	0.03822	0.05151	0.05128	0.04371
	OF_{Max}	0.03570	0.16136	0.07977	0.09141	0.06340	0.05648
	OF_{SD}	0.00384	0.03801	0.01776	0.01554	0.00517	0.00538
IV	OF_{Mean}	0.02427	0.05045	0.03373	0.04014	0.03201	0.02837
	OF_{Min}	0.02403	0.03794	0.02752	0.03111	0.02888	0.02533
	OF_{Max}	0.02455	0.06513	0.04003	0.04977	0.03488	0.02965
	OF_{SD}	0.00021	0.01237	0.00517	0.00785	0.00274	0.00175
V	OF_{Mean}	0.04136	0.11366	0.09628	0.14511	0.06885	0.08344
	OF_{Min}	0.03877	0.04128	0.06272	0.07654	0.05452	0.05560
	OF_{Max}	0.04840	0.20169	0.11964	0.21617	0.07725	0.10943
	OF_{SD}	0.00401	0.06367	0.02384	0.06441	0.00881	0.01955
VI	OF_{Mean}	0.05199	0.12077	0.14000	0.15824	0.11729	0.14098
	OF_{Min}	0.04058	0.08797	0.08657	0.07043	0.08278	0.09451
	OF_{Max}	0.06674	0.16411	0.18970	0.22823	0.13531	0.18131
	OF_{SD}	0.01007	0.02866	0.03758	0.06355	0.02080	0.03328

Table 15. Statistical analysis.

Friedman rank test						
	JOA	SCA	LJA	NMSA	SOSA	EHOA
Mean rank	1	4.83333	3	5	3.33333	3.83333
Q value	18.28571					
p value	0.002609					

Table 16. Friedman rank test.

Data availability

The datasets used and/or analyzed during the current study are available from the corresponding author upon reasonable request.

Received: 17 April 2024; Accepted: 7 May 2024

Published online: 20 May 2024

References

- Taherdoost, H. & Madanchian, M. Multi-criteria decision making (mcdm) methods and concepts. *Encyclopedia* **3**, 77–87 (2023).
- Parekh, H., Yadav, K., Yadav, S. & Shah, N. Identification and assigning weight of indicator influencing performance of municipal solid waste management using ahp. *KSCE J. Civ. Eng.* **19**, 36–45 (2015).
- Myronidis, D., Papageorgiou, C. & Theophanous, S. Landslide susceptibility mapping based on landslide history and analytic hierarchy process (AHP). *Nat. Hazards* **81**, 245–263 (2016).
- Günen, M. A. Determination of the suitable sites for constructing solar photovoltaic (PV) power plants in Kayseri, Turkey using GIS-based ranking and AHP methods. *Environ. Sci. Pollut. Res.* **28**, 57232–57247 (2021).
- Hammami, S. *et al.* Application of the GIS based multi-criteria decision analysis and analytical hierarchy process (AHP) in the flood susceptibility mapping (Tunisia). *Arab. J. Geosci.* **12**, 1–16 (2019).
- Zhou, K. Comprehensive evaluation on water resources carrying capacity based on improved AGA-AHP method. *Appl. Water Sci.* **12**, 103 (2022).
- Nyimbili, P. H., Erden, T. & Karaman, H. Integration of GIS, AHP and topsis for earthquake hazard analysis. *Nat. Hazards* **92**, 1523–1546 (2018).
- Li, M. *et al.* Groundwater quality evaluation and analysis technology based on AHP-EWM-GRA and its application. *Water Air Soil Pollut.* **234**, 19 (2023).
- Kwong, C.-K. & Bai, H. A fuzzy AHP approach to the determination of importance weights of customer requirements in quality function deployment. *J. Intell. Manuf.* **13**, 367–377 (2002).

10. Ertuğrul, İ & Karakaşoğlu, N. Comparison of fuzzy AHP and fuzzy topsis methods for facility location selection. *Int. J. Adv. Manuf. Technol.* **39**, 783–795 (2008).
11. Ayağ, Z. & Özdemir, R. G. A fuzzy AHP approach to evaluating machine tool alternatives. *J. Intell. Manuf.* **17**, 179–190 (2006).
12. Shaygan, A. & Testik, Ö. M. A fuzzy AHP-based methodology for project prioritization and selection. *Soft Computing* **23**, 1309–1319 (2019).
13. Srdjevic, B. & Medeiros, Y. D. P. Fuzzy AHP assessment of water management plans. *Water Resour. Manag.* **22**, 877–894 (2008).
14. Beskese, A., Demir, H. H., Ozcan, H. K. & Okten, H. E. Landfill site selection using fuzzy AHP and fuzzy topsis: a case study for Istanbul. *Environ. Earth Sci.* **73**, 3513–3521 (2015).
15. Karasan, A., Ilbahar, E. & Kahraman, C. A novel pythagorean fuzzy AHP and its application to landfill site selection problem. *Soft Computing* **23**, 10953–10968 (2019).
16. Mamta, et al. Rank exponent method based optimal control of AGC for two-area interconnected power systems. *IEEE Access* **12**, 35571–35585. <https://doi.org/10.1109/ACCESS.2024.3373043> (2024).
17. Krishna, P., Meena, V., Singh, V. & Khan, B. Rank-sum-weight method based systematic determination of weights for controller tuning for automatic generation control. *IEEE Access* **10**, 68161–68174 (2022).
18. Singh, S. P., Prakash, T., Singh, V. & Babu, M. G. Analytic hierarchy process based automatic generation control of multi-area interconnected power system using Jaya algorithm. *Eng. Appl. Artif. Intell.* **60**, 35–44 (2017).
19. Krishna, P., Meena, V., Patnana, N., Mathur, A. & Singh, V. Grey wolf optimizer-assisted r-method-based weighted minimization for automatic generation control in two-area interconnected power system. *Int. J. Dyn. Control* **11**, 1779–1796 (2023).
20. Ram Babu, N. et al. A comprehensive review of recent strategies on automatic generation control/load frequency control in power systems. *Arch. Comput. Methods Eng.* **30**, 543–572 (2023).
21. Bhagat, S. K. et al. A review on various secondary controllers and optimization techniques in automatic generation control. *Arch. Comput. Methods Eng.* **30**, 3081–3111 (2023).
22. Pabitra, M., Mohapatra, S. K., Baliarsingh, A. & Das, R. Application of pid controller-based automatic generation control for interconnected power system with governor dead-band non-linearity using mol algorithm. In *Advances in Energy Technology: Proceedings of ICAET 2020*, 25–35 (Springer, 2020).
23. Chintu, J. M. R. & Sahu, R. K. Differential evolution optimized fuzzy pid controller for automatic generation control of interconnected power system. In *Computational Intelligence in Pattern Recognition: Proceedings of CIPR 2020*, 123–132 (Springer, 2020).
24. Karanam, A. N. & Shaw, B. A new two-degree of freedom combined PID controller for automatic generation control of a wind integrated interconnected power system. *Protect. Control Modern Power Syst.* **7**, 20 (2022).
25. Raheem, F. S. & Basil, N. Automation intelligence photovoltaic system for power and voltage issues based on black hole optimization algorithm with fopid. *Measure. Sensors* **25**, 100640 (2023).
26. Basil, N. & Marhoon, H. M. Selection and evaluation of fopid criteria for the x-15 adaptive flight control system (AFCS) via Lyapunov candidates: Optimizing trade-offs and critical values using optimization algorithms. *e-Prime-Adv. Electric. Eng. Electron. Energy* **6**, 100305 (2023).
27. Basil, N. et al. Black-hole optimisation algorithm with FOPID-based automation intelligence photovoltaic system for voltage and power issues. *Austr. J. Electric. Electron. Eng.* 1–13. <https://doi.org/10.1080/1448837X.2024.2308415> (2024).
28. Marhoon, H. M., Basil, N. & Mohammed, A. F. Medical Defense Nanorobots (MDNRs): a new evaluation and selection of controller criteria for improved disease diagnosis and patient safety using NARMA(L2)-FOP + D(ANFIS) μ -L-based Archimedes Optimization Algorithm. *Int. J. Inform. Technol.* <https://doi.org/10.1007/s41870-023-01724-7> (2024).
29. Mohamadwasel, N. Rider optimization algorithm implemented on the AVR control system using matlab with fopid. In *IOP Conference Series: Materials Science and Engineering*, vol. 928, 032017 (IOP Publishing, 2020).
30. Basil, N. & Marhoon, H. M. Towards evaluation of the PID criteria based UAVS observation and tracking head within resizable selection by COA algorithm. *Results Control Optim.* **12**, 100279 (2023).
31. Basil, N., Marhoon, H. M. & Ibrahim, A. R. A new thrust vector-controlled rocket based on JOA using MCDA. *Measure. Sensors* **26**, 100672 (2023).
32. Basil, N., Marhoon, H. M., Gokulakrishnan, S. & Buddhi, D. Jaya optimization algorithm implemented on a new novel design of 6-DOF AUV body: a case study. *Multimed. Tools Appl.* <https://doi.org/10.1007/s11042-022-14293-x> (2022).
33. Mohammed, A. F. et al. Selection and evaluation of robotic arm based conveyor belts (RACBS) motions: Narma (l2)-fo (anf) pd-i based Jaya optimization algorithm. *Int. J. Robot. Control Syst.* **4**, 262–290 (2024).
34. Kubler, S., Robert, J., Derigent, W., Voisin, A. & Le Traon, Y. A state-of-the-art survey & testbed of fuzzy AHP (FAHP) applications. *Expert Syst. Appl.* **65**, 398–422 (2016).
35. Juang, Y.-T., Chang, Y.-T. & Huang, C.-P. Design of fuzzy PID controllers using modified triangular membership functions. *Inform. Sci.* **178**, 1325–1333 (2008).
36. Ali, E. S. & Abd-Elazim, S. M. Bacteria foraging optimization algorithm based load frequency controller for interconnected power system. *Int. J. Electric. Power Energy Syst.* **33**, 633–638 (2011).
37. Rao, R. Jaya: A simple and new optimization algorithm for solving constrained and unconstrained optimization problems. *Int. J. Indus. Eng. Comput.* **7**, 19–34 (2016).
38. Houssein, E. H., Gad, A. G. & Wazery, Y. M. Jaya algorithm and applications: A comprehensive review. In *Metaheuristics and Optimization in Computer and Electrical Engineering* (eds. Razmjooy, N., Ashourian, M. & Foroozandeh, Z.). Lecture Notes in Electrical Engineering, vol 696. https://doi.org/10.1007/978-3-030-56689-0_2 (Springer, Cham, 2021).

Author contributions

Conceptualization, T.V., A.V.W., V.P.S., V.P.M.; Methodology, T.V., A.V.W., V.P.S., V.P.M., A.R., B.K.; Software, T.V., A.V.W., V.P.S., V.P.M.; Validation, V.P.M., A.R., B.K.; Formal analysis, T.V., A.V.W., V.P.S., V.P.M., A.R., B.K.; Investigation, V.P.M., A.R., B.K.; Resources, T.V., A.V.W., V.P.S., V.P.M., A.R., B.K.; Data curation, T.V., A.V.W., V.P.S., V.P.M., A.R., B.K.; Writing— original draft, T.V., A.V.W., V.P.S., V.P.M.; Writing—review & editing, T.V., A.V.W., V.P.S., V.P.M., A.R., B.K.; Visualization, T.V., A.V.W., V.P.S., V.P.M., A.R., B.K.; Supervision, V.P.M. and B.K.; Funding acquisition, B.K. All authors have read and agreed to the published version of the manuscript.

Funding

The authors did not receive support from any organization for the submitted work.

Competing interests

The authors declare no competing interests.

Additional information

Correspondence and requests for materials should be addressed to B.K.

Reprints and permissions information is available at www.nature.com/reprints.

Publisher's note Springer Nature remains neutral with regard to jurisdictional claims in published maps and institutional affiliations.



Open Access This article is licensed under a Creative Commons Attribution 4.0 International License, which permits use, sharing, adaptation, distribution and reproduction in any medium or format, as long as you give appropriate credit to the original author(s) and the source, provide a link to the Creative Commons licence, and indicate if changes were made. The images or other third party material in this article are included in the article's Creative Commons licence, unless indicated otherwise in a credit line to the material. If material is not included in the article's Creative Commons licence and your intended use is not permitted by statutory regulation or exceeds the permitted use, you will need to obtain permission directly from the copyright holder. To view a copy of this licence, visit <http://creativecommons.org/licenses/by/4.0/>.

© The Author(s) 2024